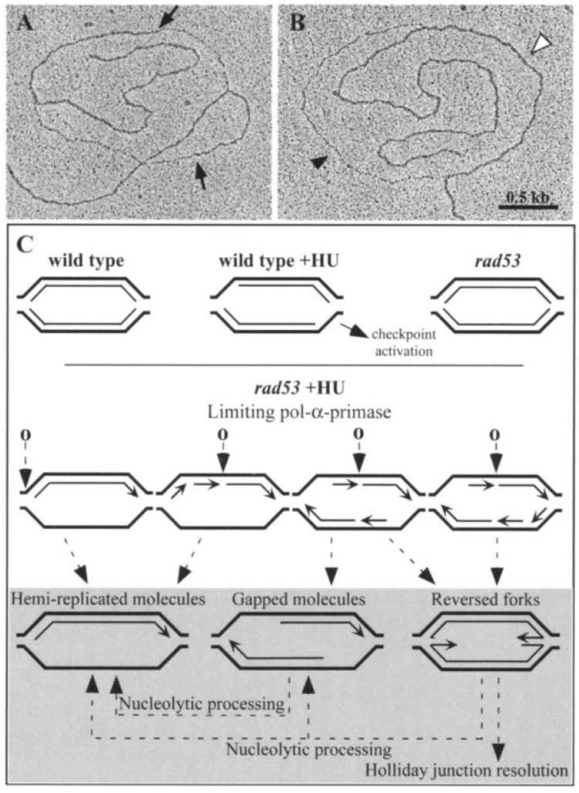

Fig. 4. DNA primase mutants accumulate hemi-replicated intermediates. Representative replicating bubbles from *pri1-M4* mutant cells (**A** and **B**) (*27*). The molecule in (A) is partially single-stranded. Arrows indicate the transition points from dsDNA to ssDNA. In (B), the white arrowhead indicates the replicated arm of a hemi-replicated bubble; the black arrowhead indicates the unreplicated strand. (**C**) Schematic representation of RIs in wild-type and *rad53* cells treated with HU or not treated. In HU-treated wild-type cells, the accumulation of short single-stranded regions likely causes checkpoint activation. In HU-treated *rad53* cells, abnormal replication intermediates, likely caused by a defect in the DNA polymerase α-primase complex, are converted into the aberrant structures represented in the gray panel. O, replication origin.

7. H. D. Lindsay *et al.*, *Genes Dev.* **12**, 382 (1998).
8. B. A. Desany, A. A. Alcasabas, J. B. Bachant, S. J. Elledge, *Genes Dev.* **12**, 2956 (1998).
9. R. Lucchini, J. M. Sogo, *Nature* **374**, 276 (1995).
10. R. Gasser, T. Koller, J. M. Sogo, *J. Mol. Biol.* **258**, 224 (1996).
11. C. Santocanale, J. F. X. Diffley, *Nature* **395**, 615 (1998).
12. K. Shirahige *et al.*, *Nature* **395**, 618 (1998).
13. B. Garvik, M. Carson, L. Hartwell, *Mol. Cell. Biol.* **11**, 6128 (1995).
14. S. E. Lee *et al.*, *Cell* **94**, 399 (1998).
15. M. B. Vaze, A. Pellicioli, M. Foiani, J. Haber, unpublished data.
16. R. B. Inmann, *Biochim. Biophys. Acta* **783**, 205 (1984).
17. M. R. Singleton, S. Scaife, D. B. Wigley, *Cell* **107**, 79 (2001).
18. M. Gruber, R. E. Wellinger, J. M. Sogo, *Mol. Cell. Biol.* **20**, 5777 (2000)
19. G. Brush, D. M. Morrow, P. Heiter, T. J. Kelly, *Proc. Natl. Acad. Sci. U.S.A.* **93**, 15075 (1996).
20. F. Marini *et al.*, *EMBO J.* **16**, 639 (1997).
21. M. Seigneur, V. Bidnenko, S. D. Ehrlich, B. Michel, *Cell* **95**, 419 (1998).
22. G. Liberi *et al.*, *EMBO J.* **19**, 5027 (2000).
23. V. Bashkirov *et al.*, *Mol. Cell. Biol.* **20**, 4393 (2000).
24. M. N. Boddy, P. Russell, *Curr. Biol.* **11**, 953 (2001)
25. J. E. Haber, W. D. Heyer, *Cell* **107**, 551 (2001).

26. We thank C. Gutierrez, J. Haber, N. Mantei, H. Mayer-Rosa, C. Newlon, P. Plevani, R. Rothstein, D. Sargent, U. Suter, F. Thoma, R. E. Wellinger, and all the members of our laboratories for discussions and support. We thank R. Cha and N. Kleckner for communicating unpublished results. This work was supported by Associazione Italiana per la Ricerca sul Cancro and partially by grants from Telethon-Italy, European Union Grant RTN2-2001-00177 and Schweizerischer Nationalfonds zur Förderung der Wissenschaflichen Forschung. M.L. was a recipient of the short-term EMBO fellowship N.9779.

Supporting Online Material
www.sciencemag.org/cgi/content/full/297/5581/599/DC1
Materials and Methods
Tables S1 to S3

26 February 2002; accepted 28 May 2002

ATR Homolog Mec1 Promotes Fork Progression, Thus Averting Breaks in Replication Slow Zones

Rita S. Cha and Nancy Kleckner*

Budding yeast Mec1, homolog of mammalian ATR, is an essential protein that mediates S-phase checkpoint responses and meiotic recombination. Elimination of Mec1 function leads to genomewide fork stalling followed by chromosome breakage. Breaks do not result from stochastic collapse of stalled forks or other incidental lesions; instead, they occur in specific regions of the genome during a G_2 chromosomal transition. Break regions are found to be genetically encoded replication slow zones (*RSZs*), a newly discovered yeast chromosomal determinant. Thus, Mec1 has important functions in normal S phase and the genome instability of *mec1* (and, analogously, *ATR*$^{-/-}$) mutants stems from defects in these basic roles.

Proteins of the ATR/ATM family (mammalian ATR and ATM, *Drosophila* mei-41, *Schizosaccharomyces pombe* rad3$^+$, and budding yeast Mec1 and Tel1) are chromosome-bound signal transduction proteins involved in DNA replication, repair, and recombination (*1*, *2*). These proteins are best understood as mediators of checkpoint responses: They sense the presence of damage or aberrations in the genome and transmit appropriate signals that trigger cell cycle arrest and coordinate repair. However, in addition, mutations in these genes confer defects during the unchallenged life of the cell. Many of these defects are also typically associated with exposure to exogenous genotoxic agents—for example, occurrence of double-strand breaks (DSBs), genome instability, and inviability. This relationship has led to a model in which potentially lethal lesions arise spontaneously during normal cellular life, with Mec1 and its homologs being required for processing of such incidental lesions (*1*, *2*). Mec1 is also involved in up-regulation of deoxynucleotide triphosphate (dNTP) synthesis through its essential downstream target Rad53, which in turn inactivates Sml1, an inhibitor of Rnr1 (*3*). Inability to up-regulate dNTP synthesis is proposed to contribute to the *mec1* phenotypes by inducing "replication stress"—that is, stalled forks that undergo irreversible collapse and/or are processed by recombination proteins into DSBs (*2*, *4*).

Alternatively, during unchallenged life, ATM/ATR/Mec1 could coordinate and promote basic chromosomal events, with the observed mutant phenotypes arising from defects in these fundamental processes, regardless of any failure to respond to incidental lesions. This notion is supported by the fact that Mec1 and its homologs are required for processes that probably occur independently of incidental damages or accidental fork stalling: the G_1 to S transition (*5*), regulation of crossover position and partner choice during meiotic recombination (*6*, *7*), and establishment of late origin firing (*8*).

Department of Molecular and Cellular Biology, Harvard University, Cambridge, MA 02138, USA.

*To whom correspondence should be addressed. E-mail: kleckner@fas.harvard.edu.

To distinguish between these two possibilities, we isolated and characterized two thermosensitive (*ts*) *mec1* alleles, *mec1-4* and *mec1-40*. Both mutations confer known *mec1* null phenotypes at nonpermissive temperature: cell inviability (Fig. 1A), absence of DNA damage checkpoint responses, and suppression of lethality by *sml1*Δ mutation. Moreover, all phenotypes are fully recessive to *MEC1*, as expected for complete loss-of-function alleles.

To characterize the defects conferred by loss of Mec1 function, we arrested *MEC1* and *mec1-ts* cells in G_1 and released them to undergo synchronous mitotic progression at nonpermissive temperature. We examined cells for DNA content by fluorescence-activated cell scanning (FACS) (Fig. 1C) and for the status of chromosome III (chrIII) by pulsed-field gel electrophoresis (PFGE) followed by end-labeling Southern analysis (Fig. 1, B, D, and E). In *MEC1*, replication initiates after 45 to 60 min. By 90 to 120 min, most cells have completed bulk DNA synthesis, as indicated by the appearance of cells containing two-cell DNA content (Fig. 1C) and reemergence of full-length linear chrIII species (Fig. 1, D to F). *MEC1* cells initiate a second round of DNA replication, as evidenced by increased retention of chrIII in the well beginning at t = 180 min. In contrast, *mec1-ts* cells exhibit prolonged replication stalling between 60 and 120 min, as indicated by the FACS profile, in which most cells exhibit intermediate DNA content, and by PFGE/Southern analysis, in which most chromosomes remain in the well (Fig. 1, D and F) in accord with the presence of branched replication intermediates (*9*). Beginning at about 150 min, chrIII emerges from the wells, giving rise to full-length linear chromosomes plus a series of discrete chrIII fragments (Fig. 1E; fig. S1B). The latter observation implies the occurrence of chromosome breaks at specific preferred positions. Chromosome fragmentation species increase in abundance and then plateau with about one break in every four chrIIIs (Fig. 1F; fig. S1C). The fragment level does not decrease, even after 24 hours, which suggests that broken ends are molecularly stable—that is, they are neither degraded nor repaired.

Concomitant with the appearance of breaks, additional changes occur (Fig. 1G; fig. S1). First, many cells acquire a general cellular catastrophe phenotype characterized by nuclear and cellular swelling plus chromatin compaction/aggregation [Fig. 1, G(a) and G(b)]. This morphology closely resembles mitotic catastrophe induced by caffeine or loss of ATR function in mammalian cells (*10*–*12*). Second, further DNA replication occurs, as evidenced by an increase in total DNA content (supporting online text). Third, cells die (Fig. 1G(c); fig. S1A). Thus, chromosome breaks in *mec1-ts* cells arise as part of a global transition involving additional DNA replication plus cellular catastrophe and death. This transition occurs well after the end of S phase, at about late G_2: Diagnostic defects appear about 40 min after cells exit the small-bud stage, which marks the end of S

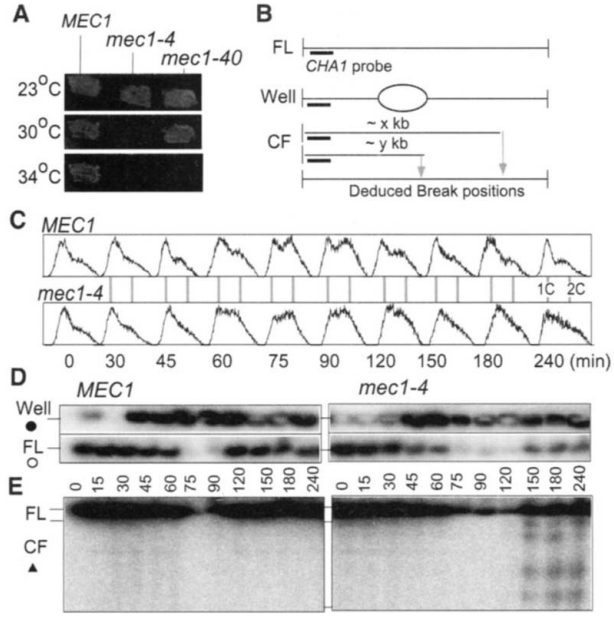

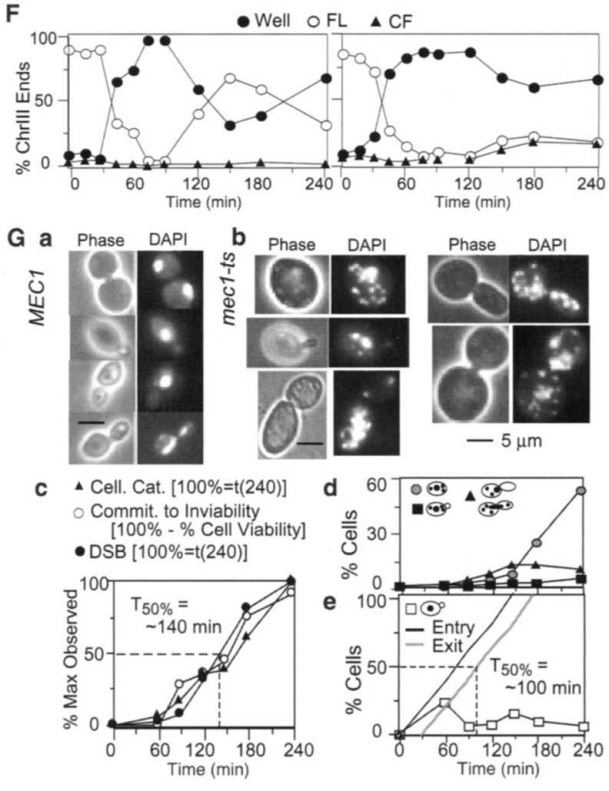

Fig. 1. *mec1-ts* phenotypes. (**A**) *mec1-ts* alleles. We incubated patches of cells (*30*) at the specified temperatures for 2 days. (**B**) ChrIII species revealed by PFGE followed by indirect labeling of one chromosome end (*CHA1*): full-length linear chromosomes ("FL"), nonlinear forms that remain in the wells of the gel ("Well") [for example, DNA replication intermediates (*9*)], and linear chromosome fragments extending from the labeled end ("CF"). Break positions along the chromosome are deduced from the lengths of CF species. (C-F) and (G) are two independent α-factor arrest/release experiments. (**C**) FACS analysis (*28*) of bulk DNA synthesis; one- and two-cell DNA contents are indicated. (**D**) PFGE/Southern analysis of chrIII (*30*). ChrIII is retained in the well concomitant with the onset of bulk DNA synthesis as assessed by FACS (C). Probe: *CHA1*. (**E**) Longer exposure of gel in (D) reveals CF species in *mec1*-4. (**F**) Fraction of hybridization signal (that is, the fraction of chromosome ends) present in each chrIII species (B). (**G**) Phase-contrast and 4',6-diamidino-2-phenylindole (DAPI) images of *MEC1* (a) and *mec1-4* (b) cells after a 4-hour incubation at 34°C. DAPI-staining entities in *mec1-4* could be nuclear and/or mitochondrial DNA. Scale bar, = 5 μm in all images. (c) By t = 140 min, about 50% of *mec1-4* cells have undergone a coordinate transition involving commitment to inviability, DSBs, and cellular catastrophe. (d) Fractions of no-bud (G_1), small-bud (S phase), and large-bud (G_2/M) *mec1-4* cells exhibiting catastrophe morphology, which first appears among G_2/M cells and then in G_1 cells. Small-bud cells exhibiting catastrophe morphology are rare throughout. (e) Fraction of *mec1-4* cells that have entered (black line) and exited (gray line) S phase is calculated from the noncumulative curve describing the fraction of S-phase cells at each time point (squares) (*28*). By t = 100 min, 50% of the cells have exited S phase.

phase in wild-type cells [compare Fig. 1G(c) with Fig. 1G(e)]; also, catastrophe occurs only in cells beyond the small-bud stage (Fig. 1G(d)).

We mapped the positions of *mec1-ts* breaks along chrIII from the lengths of the corresponding end-labeled chromosome fragments (Fig. 2, A and B). Breaks occur in about 10-kilobase (kb) "zones" in regular alternation with active replication origins (*ARS*s) except that no break region occurs between the origins that flank the centromere (Fig. 2D). This same breakage pattern is observed in both *mec-1-4* and *mec1-40* mutants, in haploid and homozygous diploid mutant strains, and in logarithmic-phase cells subjected to temperature upshift as well as cells released from α-factor arrest. Break zones are not correlated with other determinants: cohesin binding/axis-association sites (*13*), R/G-band base composition isochores that also correspond to meiotic DSB zones (Fig. 2C; fig. S2), or sites of topoisomerase II cleavage or DNase hypersensitivity (*14*). To determine whether the positions of breaks are genetically specified, we examined structural variants of chrIII in which a nonbreak-region segment was duplicated (with or without an encoded *ARS*) or in which a single *ARS* or three adjacent *ARS* elements were deleted [Fig. 2E(a)]. In all variants examined, *mec1-ts* chromosome breaks occurred at the same genetic positions as in wild-type chromosomes [Fig. 2, E(b) to E(d); fig. S3]. Thus, break positions are encoded by determinants within break zones themselves. Break zones do not represent sites of stochastic fork convergence, nor do they do arise because forks proceed a certain distance from their origins and then stall (supporting online text).

Because chromosome breakage is preceded by prolonged stalling of bulk DNA synthesis, we reasoned that break zones might represent regions of unusual replication program. Therefore, we analyzed fork progression by two-dimensional gel analysis of replication intermediates (RIs). We examined three regions that exhibit chromosome breaks and three regions that do not (Fig. 3A). In wild-type cells, RIs appear and disappear in all six segments during the period of bulk DNA replication as defined by FACS. Only Y arcs are seen, which implies the presence of unidirectional replication forks throughout each segment (Fig. 3B; fig. S4A). However, RIs are present in greater abundance in each of the three "break" segments than in the "non-break" segment examined in the same experiment, which implies that forks spend longer times in the break segments. Thus, the regions identified by *mec1-ts* breaks correspond, in wild-type cells, to regions where replication fork progression is intrinsically slow: "replication slow zones" (*RSZ*s). Genomic analysis of replication fork progression on chrIII (*15*), although less sensitive, gives patterns consistent with the current *RSZ* assignments (further discussed in supporting online text).

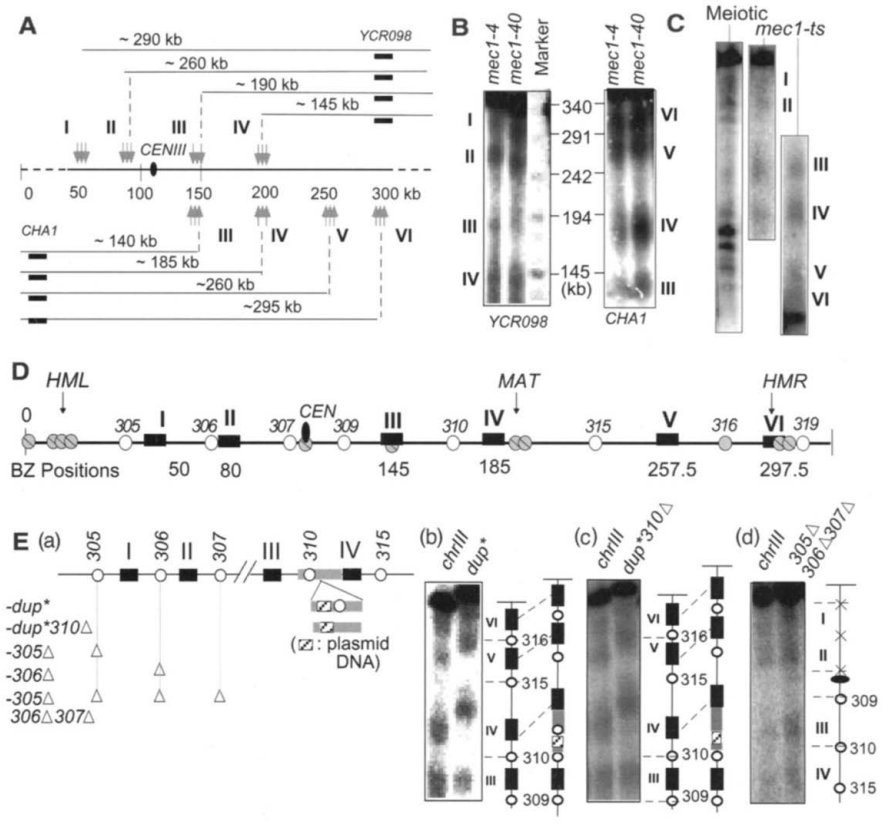

Fig. 2. *mec1-ts* break zones along chrIII. (**A** and **B**) Chromosomal breaks in *mec1-4* and *mec1-40* mutants occur in six zones (I to VI), each spanning about 10 kb. *CHA1* and *YCR098* probes identify four break zones each: III to VI and I to IV, respectively. Chromosome fragment sizes are estimated by comparison with bacteriophage λ DNA concatemers run in the same gel. Termini were not analyzable (dotted regions). DNA coordinates are from the *Saccharomyces* Genome Database (*31*). (**C**) Lack of correlation between the positions of *mec1-ts* breaks and programmed meiotic DSBs. (**D**) *mec1-ts* break zones (BZs) occur between seven highly active (open circle) and one intermediately active (gray circle) *ARS* elements along chrIII. ChrIII also contains seven minimally active origins (gray circle with line) (*15, 32*). (**E**) (a) Schematic representation of chrIII structural variants (*30*). (b to d) Break distribution in *mec1-4* strains containing wild-type or variant chrIII. Probes: *CHA1* (b and c) and *YCR098* (d).

*RSZ*s retain their basic characteristics in *mec1-ts* cells: higher levels of RIs are seen in the three break segments than in the three non-break segments (Fig. 3C; fig. S4B). Furthermore, in all six regions analyzed, RIs increase to higher levels in *mec1-ts* than in *MEC1* and remain at those high levels until the onset of the G_2 transition, as defined by the appearance of chromosome breaks; thereafter, RI levels decrease. These observations imply that Mec1 is required for progression of replication forks throughout the genome. Furthermore, they point to a causal relationship between fork stalling and chromosome breakage. In additional support for such a link, both the *mec1-ts* fork progression defect and *mec1-ts* chromosome breakage at *RSZ*s are suppressed by an *sml1*Δ mutation (Fig. 3, D to F).

Notably, RI levels in slow zones are at most about 3 times as high as in other regions, whereas chromosome breaks in slow zones are at least 5 to 7 times as high as those in intervening regions, where they are essentially undetectable. Thus, chromosome breaks occur only among the subset of forks that happen to have stalled in *RSZ*s. Chromosome breaks, along with resumption of replication (supporting online text), could be coordinate consequences of the global chromosomal transition that normally occurs in late G_2—for example, as signaled by the loss of cohesin proteins seen in yeast chrIII (*13*), as in higher eukaryotes (*16*), with *RSZ*s being especially sensitive to this transition. Alternatively, breaks might be triggered by G_2/M spindle forces (*17*). However, there is no indication that breaks occur preferentially in centromere-proximal slow zones (Fig. 2, B and C), as might be expected in the latter case.

Additional considerations suggest that, when forks stall because of the absence of

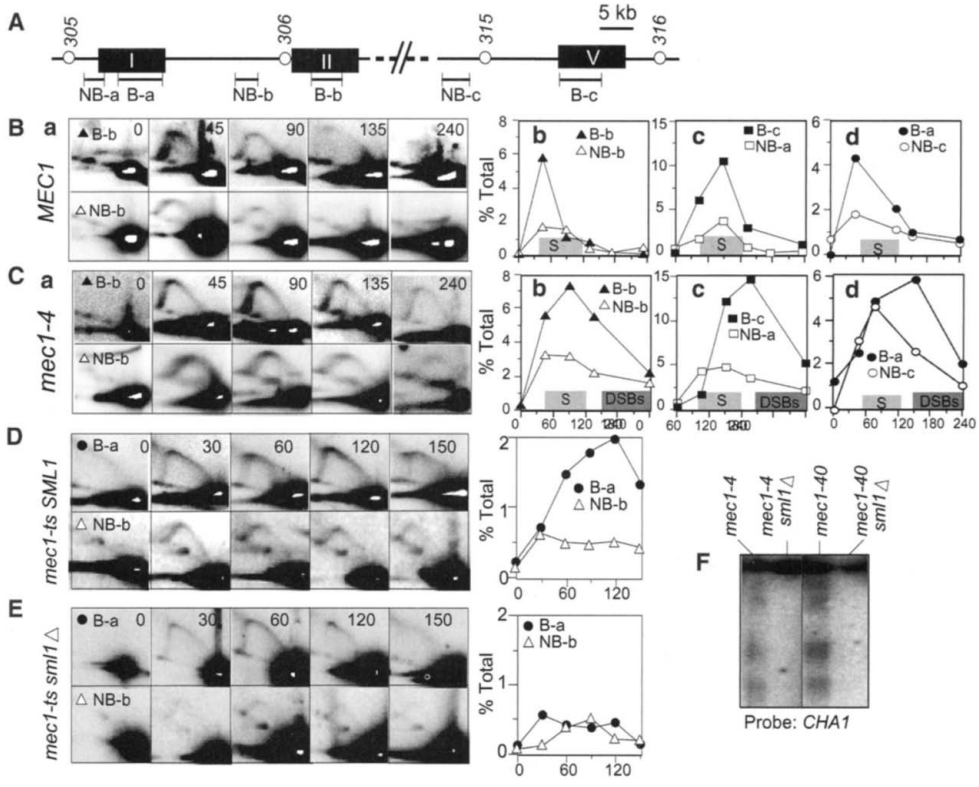

Fig. 3. Two-dimensional gel analysis of replication intermediates in break and non-break zones. (**A**) Break ("B-") and non-break-("NB-") segments are analyzed. (**B** and **C**) *MEC1* and *mec1-4* cells were α-factor arrested and released into medium containing yeast extract, peptone, and dextrose (YPD) at 34°C and replication intermediates were analyzed (*30*). (a) Two-dimensional gel patterns of segments B-b and NB-b. (b) RI signals were quantified and expressed as a fraction of total signal. (c and d) RI signals for two additional B/NB pairs (fig. S3). In each panel, both segments were assayed in the same genomic DNA sample. S, bulk DNA synthesis; DSB, presence of breaks. (**D** and **E**) Analysis of B-a and NB-b segments in *mec1-4* and *mec1-4 sml1*Δ cultures as in (B) and (C). (**F**) Status of chrIII in *mec1-ts* and *mec1-ts sml1*Δ cultures after a 4-hour incubation at 34°C.

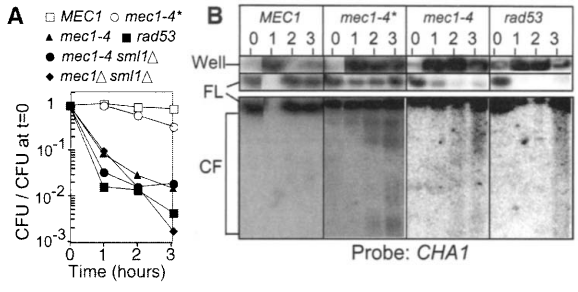

Fig. 4. Response to transient HU exposure in *mec1-ts*, *mec1*Δ, and *rad53*K277A mutants. Strains indicated, except *mec1-4**, were released from α-factor arrest into YPD medium containing HU (100 mg/ml) at 34°C. After 30 min, cells were resuspended in fresh YPD medium without HU and further incubated at 34°C. *mec1-4** cells were kept at 34°C without HU. (**A**) Relative viability. (**B**) Status of chrIII.

Mec1, they are paused in a physiologically normal state without attendant collapse. In *mec1-ts* cells exposed to hydroxyurea (HU), replication rapidly halts and cells immediately lose viability (Fig. 4). Analogous effects occur in *mec1*Δ and related checkpoint-defective mutants (*4*), providing further evidence that the *mec1-ts* mutation abrogates normal checkpoint responses. In contrast, fork stalling resulting from the absence of Mec1 during unchallenged S phase is not immediately accompanied by cell death (Fig. 4, *mec1-4**). The cell death that occurs in *mec1* in response to exogenously imposed damage can be directly attributed to replication fork collapse (*18*, *19*). By implication, fork stalling in unchallenged *mec1-ts* cells does not involve immediate replication fork collapse.

The results presented above have three important general implications. First, Mec1 plays a role in replication fork progression during normal, unchallenged S phase. Second, *mec1* chromosome breaks do not arise at the sites of stochastic fork collapse or other occasional "incidental" chromosomal lesions. Instead, breaks occur in preferred locations in the genome, after, and as a consequence of, stalling of DNA replication. Replication defects, chromosome breaks, and genome instability in corresponding mutants of other organisms (for example, $ATR^{-/-}$) would be explained by these same effects. *mec1-ts* chromosome breakage also closely resembles breakage at mammalian fragile sites, which are triggered by delayed progression through normally late-replicating regions (*20*) that also seem to be sites of naturally occurring chromosome breaks (*21*). These analogies point to possible mechanistic commonality. Third, *RSZ*s are identified as a basic chromosomal determinant that, in addition to slowing fork progression, may also serve to accumulate converging forks (supporting online text).

Why should Mec1, a chromosome-based signal transduction protein, be involved in fork progression during normal S phase? Because Mec1 is implicated in up-regulation of dNTP synthesis, the observed *mec1* phenotypes might be explained by global depletion of dNTP levels (*3*). However, this model is insufficient to explain other Mec1-related S-phase phenomena. We suggest that Mec1, together with *RSZ*s, plays a role in ensuring regular post-fork chromosome development. *RSZ*s promote periodic pausing of fork progression, thus providing time for development of important chromosomal features behind the fork—for example, installation of nucleosomes or development of intersister connections, both of which are tightly linked to replication (*22*–*24*). Mec1 would monitor installation of key features in newly replicated regions and promote progression of nearby replication forks when these events have been completed. Such activity would automatically be focused at *RSZ*s because of preferential occurrence of RIs in those regions. In support of this model, Rad53, a key downstream target of Mec1, interacts physically with Asf1, a component of the replication-dependent chromatin remodeling complex, which is needed for proper completion of DNA synthesis during normal S phase (*25*). The mechanism of such regulation remains to be determined. However, dNTPs are provided to replication forks by an allosterically coordinated multienzyme complex localized at the replisome (*26*, *27*). Perhaps Mec1 modulates fork progression by modulating the activity of this

complex, giving local pulses of dNTPs at the appropriate times.

Such an S-phase chromosome feedback system could also explain temporal programming and modulation of S-phase length. Mec1 may act in cis to promote replication fork progression and in trans to inhibit late replication origin firing as well as S-phase exit. If Mec1-mediated fork progression were accompanied by coordinate alleviation of the two trans inhibitory effects, orderly progression of replication and post-fork development throughout the genome could be ensured; once all forks are resolved, the cell would exit S phase. Moreover, the length of S phase could be expanded or contracted as an integral process without altering either the number or the pattern of fired origins or the intrinsic rate of fork progression. Instead, the length of S phase could be governed by the rate of post-fork chromosome morphogenesis. Correspondingly, meiotic S phase appears to be an expanded version of mitotic S phase, and its length is modulated positively by meiotic cohesin Rec8 and negatively by meiotic pairing/recombination protein Spo11 (*28*). This model also explains why Mec1 (via Rad53) is a negative regulator of late-origin firing in unchallenged cells (*8*) and predicts that a *rad53* mutant should exhibit longer than normal S phase despite its early firing of late origins because of its inability to promote fork progression through *RSZs*. We observe exactly this effect in both mitosis and meiosis (supporting online text).

Throughout the mitotic and meiotic programs, chromosomal changes must occur in a regulated way throughout the genome, different chromosomal events must be coordinated with one another, and progression of the cell cycle must be linked to proper completion of such processes. We suggest that ATR/ATM-family proteins mediate such effects, not only during S phase but also potentially during G_1 (*5*), meiotic prophase (*6*, *7*), and in the cytoplasm, where ATM mediates signal transduction during normal cellular responses (*29*). Failure to carry out certain of these basic roles then contributes to the defects observed in the corresponding mutants in the absence of exogenous insult. By this view, DNA damage/replication checkpoint responses could represent specialized amplifications and applications of functions having more basic roles.

References and Notes

1. R. Abraham, *Genes Dev.* **15**, 2177 (2001).
2. B. B. Zhou, S. J. Elledge, *Nature* **408**, 433 (2000).
3. X. Zhao, A. Chabes, V. Domkin, L. Thelander, R. Rothstein, *EMBO J.* **20**, 3544 (2001).
4. B. Desany, A. A. Alcasabas, J. B. Bachant, S. J. Elledge, *Genes Dev.* **12**, 2956 (1998).
5. Y. Xu, D. Baltimore, *Genes Dev.* **10**, 2401 (1996).
6. B. Baker, A. Carpenter, *Genetics* **71**, 255 (1972).
7. J. M. Grushcow, T. M. Holzen, K. J. Park, T. Weintert, M. Licheten, D. K. Bishop, *Genetics* **153**, 607 (1999).
8. K. Shirahige *et al.*, *Nature* **395**, 613 (1998).
9. K. Hennessy, A. Lee, E. Chen, D. Botstein, *Genes Dev.* **5**, 958 (1991).
10. R. Schlegel, A. Pardee, *Science* **232**, 1264 (1986).
11. P. Nghiem, P. Park, Y. Kim , C. Vaziri, S. Schreiber, *Proc. Natl. Acad. Sci. U.S.A.* 9029 (2001).
12. E. Brown, D. Baltimore, *Genes Dev.* **14**, 397 (2000).
13. Y. Blat, N. Kleckner, *Cell* **98**, 249 (1999).
14. V. Borde, T.-C. Wu, M. Lichten, *Mol. Cell Biol.* **19**, 4832 (1999).
15. M. Raghuraman *et al.*, *Science* **294**, 115 (2001).
16. I. Waizenegger, S. Hauf, A. Meinke, J. Peters, *Cell* **103**, 399 (2000).
17. D. Thrower, K. Bloom, *Mol. Biol. Cell* **12**, 2800 (2001).
18. M. Lopes *et al.*, *Nature* **412**, 557 (2001).
19. J. Tercero, J. Diffley, *Nature* **412**, 553 (2001).
20. C. Laird, R. Hansen, T. Canfield, M. Lamb, S. Gartlers, *Cold Spring Harbor Symp. Quant. Biol.* **58**, 633 (1993).
21. G. Sutherland, F. Hecht, *Fragile Sites on Human Chromosomes*. Oxford Monographs on Medical Genetics (Oxford Univ. Press, New York, 1985).
22. K.-I. Shibahara, B. Stillman, *Cell* **96**, 576 (1999).
23. A. Toth, R. Ciosk, F. Uhlmann, M. Galova, A. Schleiffer, K. Nasmyth, *Genes Dev.* **13**, 320 (1999).
24. R. V. Skibbens, L. B. Corson, D. Koshland, P. Hieter, *Genes Dev.* **13**, 307 (1999).
25. S. Le, C. Davis, J. Konopka, R. Sternglanz, *Yeast* **13**, 1029 (1997).
26. C. Mathews, *Prog. Nucleic Acids Res.* **44**, 167 (1993).
27. G. Reddy, A. Pardee, *Nature* **304**, 86 (1983).
28. R. Cha, B. Weiner, S. Keeney, J. Dekker, N. Kleckner, *Genes Dev.* **14**, 493 (2000).
29. D. Yang, M. Kastan, *Nature Cell Biol.* **2**, 893 (2000).
30. Materials and methods are available as supporting material on *Science* Online.
31. http://genome-www.stanford.edu/Saccharomyces/
32. A. Poloumienko, A. Dershowitz, J. De, C. Newlon, *Mol. Biol. Cell* **12**, 3317 (2001).

33. Supported by NIH grant (GM25326) to N.K. We thank M. Lichten, C. Newlon, H. Ogawa, and D. Stern for plasmids and strains and D. Bishop, M. Foiani, and the Kleckner laboratory for critical reading of the manuscript.

Supporting Online Material

www.sciencemag.org/cgi/content/full/297/5581/602/DC1
Materials and Methods
Supporting Text
Figs. S1 to S4

28 February 2002; accepted 7 May 2002

Biallelic Inactivation of *BRCA2* in Fanconi Anemia

Niall G. Howlett,[1] Toshiyasu Taniguchi,[1] Susan Olson,[2] Barbara Cox,[2] Quinten Waisfisz,[3] Christine de Die-Smulders,[4] Nicole Persky,[1] Markus Grompe,[2] Hans Joenje,[3] Gerard Pals,[3] Hideyuki Ikeda,[5] Edward A. Fox,[1] Alan D. D'Andrea[1]*

Fanconi anemia (FA) is a rare autosomal recessive cancer susceptibility disorder characterized by cellular hypersensitivity to mitomycin C (MMC). Six FA genes have been cloned, but the gene or genes corresponding to FA subtypes B and D1 remain unidentified. Here we show that cell lines derived from FA-B and FA-D1 patients have biallelic mutations in *BRCA2* and express truncated BRCA2 proteins. Functional complementation of FA-D1 fibroblasts with wild-type *BRCA2* complementary DNA restores MMC resistance. Our results link the six cloned FA genes with *BRCA1* and *BRCA2* in a common pathway. Germ-line mutation of genes in this pathway may result in cancer risks similar to those observed in families with *BRCA1* or *BRCA2* mutations.

Fanconi anemia (FA) is a rare autosomal recessive cancer susceptibility syndrome characterized by congenital abnormalities, progressive bone marrow failure, and cellular hypersensitivity to DNA cross-linking agents, such as MMC and cisplatin (*1*, *2*). FA patients often develop acute myeloid leukemia (AML), but also develop squamous cell carcinomas, frequently of the head and neck or of the gynecologic system (*3*). Whether heterozygote carriers of FA gene mutations have an increased cancer risk remains unknown (*4*).

At least eight distinct complementation groups of FA (A, B, C, D1, D2, E, F, G) have been defined by somatic cell fusion studies (*5*–*7*), and six FA genes have been cloned (A, C, D2, E, F, G). The six known FA proteins interact in a common pathway (*8*). Five of the FA proteins (A, C, E, F, G) assemble in a multisubunit nuclear complex. Either in response to DNA damage (*8*) or during S phase of the cell cycle (*9*), this complex activates the monoubiquitination of the downstream D2 protein, thereby targeting D2 to BRCA1-containing nuclear foci. Biallelic mutation of an upstream FA gene disrupts the monoubiquitination of FANCD2, resulting in loss of

[1]Department of Pediatric Oncology, Dana-Farber Cancer Institute and Department of Pediatrics, Children's Hospital, Harvard Medical School, 44 Binney Street, Boston, MA 02115, USA. [2]Department of Molecular and Medical Genetics and Department of Pediatrics, Oregon Health Sciences University, Portland, OR 97201, USA. [3]Department of Clinical Genetics and Human Genetics, Free University Medical Center, Van der Boechorststraat 7, NL-1081 BT Amsterdam, The Netherlands. [4]Department of Clinical Genetics, Academic Hospital Maastricht, Maastricht, Netherlands. [5]Department of Pathology, Sapporo Medical University School of Medicine, S-1, W-17, Chuo-ku, Sapporo 060-8557, Japan.

*To whom correspondence should be addressed. E-mail: alan_dandrea@dfci.harvard.edu